

## UV dominant optical emission newly detected from radioisotopes and XRF sources

M. A. Padmanabha Rao

*Charak Sadan, Vikaspuri, New Delhi 110018, India*

(Received on 21 September, 2009)

The current paper reports first and definite experimental evidence for  $\gamma$ -, X-, or  $\beta$  radiation causing UV dominant optical radiation from (1) radiochemicals such as  $^{131}\text{I}$ ; (2) XRF sources such as Rb XRF source present as salts; and (3) metal sources such as  $^{57}\text{Co}$ , and Cu XRF sources. Due to low quantum yield a need arose to develop two techniques with narrow band optical filters, and sheet polarizers that helped in the successful detection of optical radiation. The metal  $^{57}\text{Co}$  spectrum observed at room temperature hinted that it could be optical emission from excited  $^{57}\text{Co}$  atoms by a previously unknown phenomenon. In order to explain UV emission, it was predicted that some eV energies higher than that of UV, termed temporarily as Bharat radiation are generated within the excited atom, while  $\gamma$ -, X-, or  $\beta$  radiation passes through core-Coulomb field. In turn, the Bharat energy internally produced within the excited atom causes UV dominant high-energy spectrum by valence excitation. As excited atoms become free from surrounding unexcited atoms by valence excitation, room temperature atomic spectra of solid radioisotopes and XRF sources became a possibility. It implies existence of temporary atomic state of solids. The experimental evidence that  $\gamma$ -, X-, and  $\beta$  radiations causing UV dominant optical emission from within excited atoms of radioisotopes suggests the possibility for solar  $\gamma$ -, X-, and  $\beta$  radiations causing EUV by the atomic phenomenon described here.

Keywords: Radioisotopes; XRF sources; Optical emission; Atomic spectra; Atomic phenomenon; Solar EUV

### I. INTRODUCTION

Radioisotopes and XRF sources came to be known as ionizing radiation sources ever since their discoveries a century ago, in the absence of reported literature on any non-ionizing radiation emission from these sources either by an experimental evidence or theoretical prediction. In this difficult situation, the current paper mainly reports first and definite experimental evidence for UV dominant optical radiation, from both radioisotopes and XRF sources. Critical analysis of experimental data strongly suggested that it is nothing but optical emission from excited atoms of the radioisotopes and XRF sources. In order to justify that it is truly an emission, the most plausible phenomenological explanation is briefly given at the end of this paper. Truly speaking, a surprise finding led to the exhaustive study reported here. There are valid reasons why the emission has evaded all these years from previous scientists. Firstly, the dominant UV not only invisible like ionizing radiations but also follow the later from one and the same source. Secondly, the emission is of low quantum yield such that the conventional atomic spectrometer was of no avail in its detection. However, the two optical techniques specially designed and developed for low light yield doubly ensured optical radiation from both radioisotopes and XRF sources. These techniques helped in distinctly identifying optical component from ionizing radiations. There is a valid reason why the emission has evaded from the previous users of Gamma-ray Spectrometer fitted with a bare photomultiplier tube (PMT) as liquid scintillation detector etc. Successful UV detection demands setting gain of the linear amplifier slightly higher than what is normally required to a scintillation detector.

The experimental set up is nothing but a simple Gamma-ray Spectrometer. Instead of scintillation detector, use of a bare photomultiplier tube (PMT) fitted with a preamplifier in the current study helped in detection of light directly from the sources. Previously, we have used in our laboratory a bare photomultiplier tube (9635QB, Thorn EMI) fitted with a preamplifier as a light sensor to test the efficacy of vari-

ous scintillation materials [1]. When bare PMT was used to test locally developed thin film scintillators with beta emitters, it has been found to be a beta sensor [2]. However, when gain of the linear amplifier was set to be slightly higher than what is required for a scintillation detector performance of the PMT differed very much with radioisotopes and XRF sources, while background level remained optimum around 12 cps. Of all the radioisotopes and XRF sources tested, Rb XRF source (AMC 2084, U.K.) amazingly showed 125 381 cps instead of the expected 8800 Rb X-ray photon yield sec<sup>-1</sup> steradian<sup>-1</sup>. Although bare PMT is an efficient light sensor, optical radiation was the least expected from an ionizing radiation source in the absence of prior theory or any experimental study on the subject. Various experiments ensued to get the clue for the unaccountable counts noted. Ultimately, a steep fall to 59 cps from 125 381 cps noticed on interposing a thin black polyethylene sheet in between the source and PMT. The insight has hinted that Rb X-rays might be causing optical radiation from Rb XRF source, demanding confirmation by a full proof method.

Atomic Spectrometer was of no avail in testing Rb XRF source due to its possible low light yield, and the need to test it at room temperature. Therefore, the author had to develop two decisive optical techniques to verify the suspected low light yield from Rb XRF source, other XRF sources, and radioisotopes. As the spectral data obtained with narrow band optical filters provide direct evidence on optical emission, presented first in this paper. Rb XRF source was tested for any optical intensity at 330, 350, 365, 383, 400, 500, 600, 650, 700, 750, 800, and 850 nm peak wavelengths in terms of counts per sec (cps). These filters have provided definite evidence for unprecedented high-energy spectrum with UV dominance as a spectral feature of Rb XRF source present in the form of solid salt (see Fig. 1 in Ref. [3]). Surprisingly, Ba XRF source (AMC 2084, U.K.), and all the radiochemicals tested including  $^{22}\text{Na}$ ,  $^{57}\text{Co}$ ,  $^{60}\text{Co}$ ,  $^{133}\text{Ba}$ ,  $^{137}\text{Cs}$ ,  $^{204}\text{Tl}$ , and  $^{241}\text{Am}$ ; and metal  $^{57}\text{Co}$  also exhibited analogous high-energy spectra.

The second technique using a pair of dichroic visible light linear polarizers confirmed the high energy spectra of radio-

chemicals, XRF sources, and metal  $^{57}\text{Co}$  from measurements of UV (up to 400 nm), visible (400 to 710 nm), and near infrared (beyond 710 nm) radiation intensities [4-6]. The experimental technique described in the current paper is the same in Refs. [4, 6]. Table 1 in Ref. 4 lists all the 21 radioisotopes and six XRF sources tested showing optical radiation. The  $^{99m}\text{Tc}$  subsequently tested also showed UV dominant optical radiation (Table 1 in Ref. [6]). Sheet polarizers have provided key information that the nature of optical spectrum of any source depends upon energy of its abundant ionizing radiation. Polarizers confirmed that both radioisotopes and XRF sources emit mostly UV radiation, as high as 83.36% to 99.62% in the gross light intensity, as spectral feature. All this information helped in explaining optical emission.

In nut shell, both the techniques doubly ensured UV dominant optical radiation from all the sources tested. However, a need arose to understand the true nature of the optical radiation commonly detected from (1) radiochemicals such as  $^{137}\text{Cs}$ , (2) XRF sources present as salts, and (3) metal  $^{57}\text{Co}$ . These insights can be of fundamental significance to the subjects of nuclear physics, X-ray physics, atomic spectroscopy, and Solar physics. However, optical spectra with UV dominance as spectral feature of the radioisotopes and XRF sources differ much from familiar luminescence [7, 8]. From this key information it was realized that the radiation did not arise from materials around the source but directly from the source itself as optical emission. A further clue has come from metal  $^{57}\text{Co}$  spectrum at room temperature. The insight pinpointed that ionizing radiation might be causing atomic emission spectrum from the parent excited  $^{57}\text{Co}$  atom by a previously unknown phenomenon. Since atomic spectra of solids (solid radioisotopes and XRF sources) are new to literature, a valid explanation became absolutely necessary.

First of all, it became necessary to explain the origin of energies responsible for valence excitation causing these atomic spectra. Unlike the basic atomic spectra caused by thermal energies [9, 10], some exciting energies generated internally within excited atom seemed to be causing these room temperature UV dominant atomic spectra. Therefore, the author has postulated that  $\gamma$ -, X-, or  $\beta$  radiation energies at keV or MeV level generate some eV energies higher than that of UV within the parent excited atom. For example, Rb X-rays may generate wavelengths 12.87 to 47.488 nm lying in between X-ray and optical spectra. Since these wavelengths do not belong to either X-rays or light, they were termed temporarily as Bharat Radiation for convenience in Refs. [3, 6]. Citing the author's research work, Carlos Austerlitz et al recently described that production of light including Bharat energy following X-rays can excite the electrons and enhances the Fricke dosimeter response [11].

Understandably, environment of excited atoms in solid radioisotopes and XRF sources that cause UV dominant optical spectra differs much from that of thermally excited atoms in gaseous phase causing the basic atomic spectra. However, atomic spectra of solid radioisotopes and XRF sources can really happen when excited atoms become free from surrounding unexcited atoms. It seems, formation of free atoms occurs due to valence excitation by Bharat radiation. All those free atoms constituting a temporary atomic state of solids seemed to be responsible for the room temperature atomic emission spectra of solid radioisotopes and XRF sources [3]. An ex-

cited atom may remain as free atom, during valence excitation resulting into fluorescent light emission, and return to ground state. It is the hope that the current study may prompt detailed investigations into the characteristics of this new form of matter and atomic spectroscopy of radioisotopes and XRF sources for further progress.

Unlike the basic atomic spectra caused by thermal energy from an external source, the current spectra are caused by energy higher than that of UV internally produced by ionizing radiation within excited atom itself. For this reason, UV dominant atomic spectra of ionizing radiation sources widely differed from basic atomic spectra. Analysis of spectral data pinpointed that the nature of atomic spectrum of any source depends purely upon its ionizing radiation energy regardless of the type of radiation, atomic number Z, and nature of source medium whether salt or metal. In nut shell, the current study describes ionizing radiations successively generate two low energy electromagnetic radiation emissions at eV level: Bharat (predicted) and optical emissions from within excited atoms of radioisotopes, and XRF sources. The current paper also briefly describes the most plausible phenomenological explanation on generation of exciting energy, which in turn causing UV dominant high- energy spectrum by valence excitation. The current paper has mentioned  $^3\text{H}$  is an exception that did not give rise to any optical emission. According to the phenomenon described in this paper, core electrons should occupy a minimum of two orbits to observe the optical emission. Probably, absence of optical emission from  $^3\text{H}$  might support the validity of the phenomenon. Essentially, degradation of keV or MeV energies to eV level taking place within an excited atom might be the reason why atomic optical emission of light was observed from both salts as well as metals.

The current experimental results on  $\gamma$ -, X-, and  $\beta$  radiations causing UV dominant optical emission from excited atoms of radioisotopes suggest a strong possibility of solar  $\gamma$ -, X-, and  $\beta$  radiations causing EUV lines in Solar flares [3]. The UV emission detected from radioisotopes and XRF sources has bearing in radiation biology in contributing more radiation dosage to patients of Radiotherapy and Nuclear Medicine than expected [6].

## II. EXPERIMENTAL

### A. Radioisotopes and XRF sources

The Board of Radiation and Isotope Technology, Mumbai, India has supplied the radioisotopes in kBq or MBq activities. Prior to the study, removed the thin opaque Mylar film served to seal planchet containing radiochemical so as to prevent its possible absorption of UV originating from source. Variable Energy X-ray Source (AMC 2084, U.K.) provided Rb, Ba, and Tb XRF sources, and metal Cu, Mo, and Ag XRF sources employed in the study.

## B. Equipment

The experimental set up is nothing but a simple Gamma Ray Spectrometer with a difference in its probe [1, 2, 4, 6]. Unexpected detection of UV dominant optical radiation owes to the use of bare PMT (9635QB, Thorn EMI) on which the source was directly kept, setting gain of the linear amplifier relatively higher than the requirement for a scintillation detector and time constant at  $0.1 \mu\text{s}$  [4, 6]. To avoid spurious counts due to possible light leak to the PMT, kept the probe consisting of a bare PMT tube coupled to a preamplifier in a sealed metal container in turn in a lead castle. Moreover, terminated the high voltage supply prior to opening the metal casing intended for source replacement, and conducted the experiments in darkness. Despite high gain setting, the optimally low background rate (12 cps) of the PMT noticed throughout the experiments ensured its satisfactory operating condition free from any light leak. Ultimately, 8K MCA displayed a single pulse height spectrum for simultaneously detected optical and ionizing radiations by thin quartz window of the PMT. Ultimately, Table 1 displays counts per second (cps) for the integral counts accrued for 4 min. Suspected low quantum yield from the calibration sources and the need to test them at room temperature did not allow drawing line spectra by Atomic Spectrometer. Addressing the limitation, the author has developed two decisive techniques useful in the situation of low light yield.

## C. Two optical techniques

### 1. Using narrow band optical filters

Manual use of narrow band optical filters was opted to verify optical intensities, if any, at 330, 350, 365, 383, 400, 450, 500, 550, 600, 650, 700, 750, 800, and 850 nm peak wavelengths in terms of counts per sec (cps). First, background level of the bare PMT has been just 12 cps on keeping the 600 nm filter directly on its quartz window. Next, on keeping Rb XRF source (AMC 2084, U.K.) on the filter noted a marginal raise of 16 cps to 28 cps, owing to poor efficiency of PMT to Rb X-rays and poor NIR radiation intensity at 600 nm peak wavelength (Fig.1). Likewise, counts remained low at 650, 700, 750, 800, and 850 nm indicating poor efficiency of PMT to Rb X-rays and poor intensity in the spectral near infrared (NIR) region. However, significant rise to 330 cps at 450 nm, and 356 cps at 400 nm provided concrete evidence for low intense emission in the spectral visible (VIS) region. In the spectral UV region, a steep rise to 852 cps at 383 nm, 710 cps at 365 nm, 3095 cps at 350 nm, and 2527 cps at 330 nm provided concrete evidence for UV emission with maximum intensity, while contribution by Rb X-rays remained below 16 cps. On plotting this data as shown in Fig.1, strong peak intensity lines in spectral UV region have indicated an unprecedented UV dominant high-energy spectrum of Rb XRF source, unlike the known strongest air wavelengths of rubidium at 424.440 nm (Rb II), and 780.027 nm (Rb I) in basic Rb atomic spectrum [9,10].

Spectral data of  $^{137}\text{Cs}$ ,  $^{60}\text{Co}$ , Rb XRF source, and metal  $^{57}\text{Co}$  in Fig.1 exemplify UV dominance as the spectral fea-

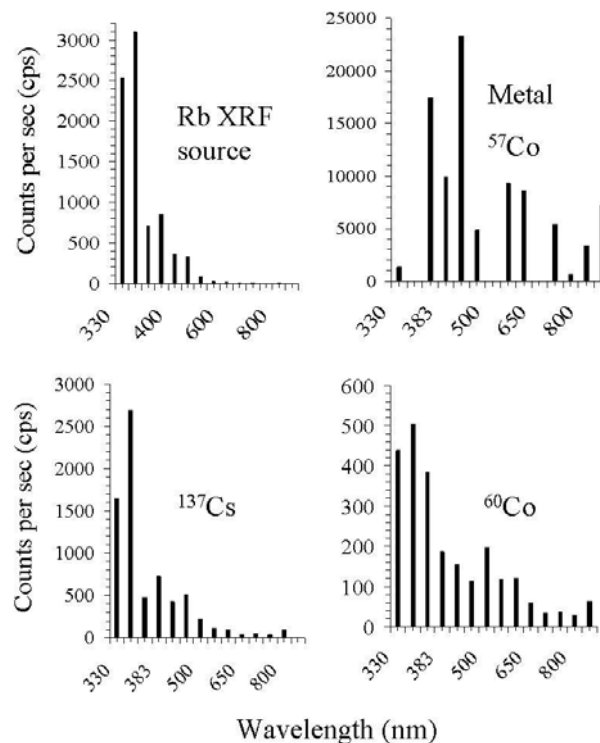


FIG. 1: First and definite experimental evidence for UV dominant optical spectra of Rb XRF source, metal  $^{57}\text{Co}$  source (notably at room temperature),  $^{137}\text{Cs}$ , and  $^{60}\text{Co}$  from peak intensity measurements made with narrow band optical filters at 330, 350, 365, 383, 400, 450, 500, 550, 600, 650, 700, 750, 800, and 850 nm peak wavelengths.

ture of ionizing radiation sources. Like metal  $^{57}\text{Co}$ , metal Cu XRF source also has shown UV dominance (see Fig.1 in Ref. [3]). Analogous UV dominant high energy spectra were also observed from Ba, and Tb XRF sources (salts); radiochemicals such as  $^{22}\text{Na}$ ,  $^{57}\text{Co}$ ,  $^{133}\text{Ba}$ ,  $^{204}\text{Tl}$ , and  $^{241}\text{Am}$ . The optical spectra of Rb XRF source, metal  $^{57}\text{Co}$ , radiochemicals  $^{137}\text{Cs}$ , and  $^{60}\text{Co}$  shown in Fig.1 reveal that X-,  $\gamma$ -, or  $\beta$  radiation can independently cause a high-energy spectrum. Precisely, the energy of abundant ionizing radiation is responsible for the differences noticed between any two spectra in Fig.1. At the same time, better understanding of high-energy spectra from three types of ionizing radiation sources: (1) radiochemicals, (2) XRF sources present as salts, and (3) radioisotopes, and XRF sources present as metals demanded further information.

### 2. Using a pair of sheet polarizers

The second technique useful in the situation of low light yield had to be developed with a pair of sheet polarizers to confirm the optical radiation observed from radioisotopes and XRF sources with narrow band optical filters. Transmission spectra of a pair of dichroic visible light linear polarizers were tested prior to their use in the technique, as can be seen in Refs. [4, 6]. The polarizers set as parallel pair show blockage of UV radiation up to 400 nm but transmission of low percent linear polarized visible (VIS) light from 400 to 710 nm and rapidly increasing NIR radiation from nearly 710 nm onwards. The polarizers, set as crossed pair, excellently

block visible light but transmit NIR radiation beyond 710 nm. These characteristics helped to estimate UV, VIS, and NIR radiation intensities from a radioisotope or XRF source. The following technique demonstrates how the UV, VIS, and NIR radiation intensity estimates could be made from metal  $^{57}\text{Co}$ .

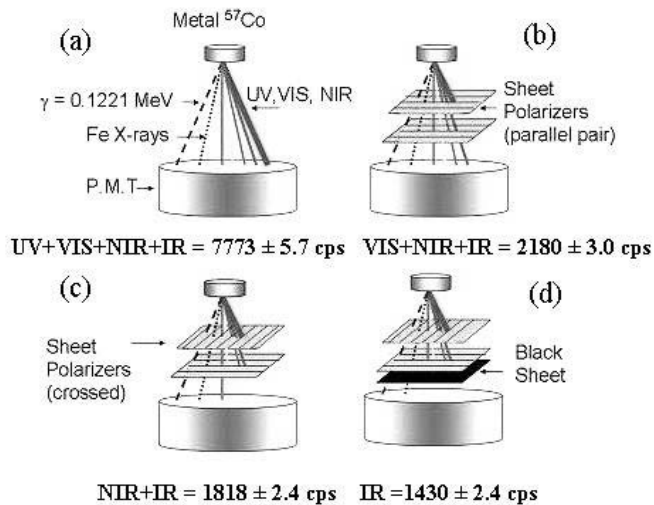


FIG. 2: Schematic of the technique developed with a pair of sheet polarizers illustrating UV dominant optical emission of metal  $^{57}\text{Co}$ , kept directly on quartz window of a bare Photomultiplier Tube (9635QB, Thorn EMI). (a). The bare PMT detected  $7773 \pm 5.7 \text{ cps}$  from  $^{57}\text{Co}$  source, owing to UV (up to 400 nm), VIS (400 - 710 nm), NIR (beyond 710 nm) radiations, and  $\gamma$ -ray as well as Fe X-ray (IR) intensities. (b): On inserting a parallel pair of polarizers in between PMT and source, counts dipped sharply due to blockage of UV from source, yet VIS, and NIR radiation intensities from 400 nm onwards together with IR caused  $2180 \pm 3.0 \text{ cps}$ . (c): When polarizers were reset as crossed pair, counts dipped further due to blockage of even linearly polarized visible (VIS) light, however NIR radiation from 710 nm onwards and IR caused  $1818 \pm 2.4 \text{ cps}$ . (d): On inserting a 0.26 mm thin black polyethylene sheet in between crossed polarizers and PMT, a further dip in counts was evident due to blockage of NIR radiation, yet IR alone caused  $1430 \pm 2.4 \text{ cps}$ . IR represents ionizing radiations.

UV, VIS, and NIR radiation intensities from  $^{57}\text{Co}$  were estimated simply from the differences in counts between four successive steps, considering IRS contribution ( $1430 \pm 2.4 \text{ cps}$ ) remains nearly the same in all four steps as the dominant gamma rays penetrate well through polarizers and polyethylene sheet.

Steps (a) - (b) = UV radiation intensity =  $5593 \pm 8.7 \text{ cps}$  (88.18 %).

Steps (b) - (c) = VIS radiation intensity =  $362 \pm 5.4 \text{ cps}$  (5.71 %)

Steps (c) - (d) = NIR radiation intensity =  $388 \pm 4.8 \text{ cps}$  (6.11%)

Gross light intensity (UV+VIS+NIR intensities) =  $6343 \pm 8.1 \text{ cps}$  (Table I).

Previously, UV, VIS, and NIR radiation intensities were shown in terms of counts [4, 6]. In Table I here, the intensity

estimates are better shown as percent of the gross light intensity to address the problem of unequal source strengths and different standard units of radioisotopes and XRF sources. In metal  $^{57}\text{Co}$  spectrum, UV intensity was as high as 88.18 % of gross light intensity, while VIS, and NIR radiation intensities remained low at 5.71% and 6.11% respectively (Table 1). Both Fig. 1 and Table I doubly ensure high-energy spectra with UV dominance as characteristic emissive feature of radioisotopes and XRF sources. A comparison of spectral data shown in Fig.1 and Table I shows that the presence of more number of peak intensity lines in spectral UV region is responsible for raise in %UV intensity of the sources when tested with polarizers. The intensity estimates in Table I were found reproducible with reasonable consistency, on repetition of experiments. High-energy spectra of metal Cu, Mo, and Ag XRF sources, Tb XRF source present in the form of Tb salt; and  $^{55}\text{Fe}$ , could not be ascertained for want of higher strength. It was also not possible to ascertain high-energy spectrum of  $^{60}\text{Co}$  metal pellet, for want of fixation in a planchet for safe handling.

TABLE I. UV dominant optical emission from (1) Rb and Ba XRF sources, (2) radiochemicals such as  $^{113}\text{Sn}$ , and (3) metal  $^{57}\text{Co}$  is evident from the columns on %UV, %VIS, and %NIR intensities in the gross light intensity measured with a pair of sheet polarizers. Likewise, optical emission from metal sources: Cu, Mo, and Ag XRF sources, and  $^{60}\text{Co}$  is evident from the gross light intensity.

Source	Most abundant emission	Energy (MeV)	gross light intensity (cps)	UV %	VIS %	NIR %
1. Sources present as chemicals						
$^{55}\text{Fe}$	Mn X-rays	0.005899	$125 \pm 0.9$			
Rb XRF	Rb X-rays	0.013336	$125322 \pm 23$	99.62	0.37	0.01
$^{113}\text{Sn}$	In X-rays	0.02421	$91105 \pm 23$	96.95	2.21	0.84
$^{133}\text{Ba}$	Cs X-rays	0.03097	$2803 \pm 3.9$	97.51	1.46	1.03
Ba XRF	Ba X-rays	0.031817	$2064 \pm 7.3$	95.64	3.83	0.53
$^{152}\text{Eu}$	Sm X-rays	0.04012	$3052 \pm 6.2$	90.33	5.9	3.77
Tb XRF	Tb X-rays	0.04423	$37 \pm 1.1$			
$^{241}\text{Am}$	$\gamma$	0.05954	$1678 \pm 2.1$	98.03	1.91	0.06
$^{201}\text{Tl}$	Hg X-rays	0.07082	$1830 \pm 2.8$	95.73	3.83	0.44
$^{57}\text{Co}$	$\gamma$	0.1221	$626 \pm 1.8$	96.01	1.76	2.23
$^{99\text{m}}\text{Tc}$	$\gamma$	0.141	$468 \pm 4.5$	94.02	3.85	2.13
$^{147}\text{Pm}$	$\beta$	0.2245	$3606 \pm 3.9$	99.36	0.58	0.06
$^{45}\text{Ca}$	$\beta$	0.253	$2333 \pm 3.2$	95.76	4.20	0.04
$^{141}\text{Ce}$	$\beta$	0.444	$727 \pm 0.9$	98.76	1.10	0.14
$^{22}\text{Na}$	$\gamma$	0.511	$2284 \pm 3.5$	94.92	2.50	2.58
$^{137}\text{Cs}$	$\beta$	0.514	$8579 \pm 7$	96.81	0.85	2.34
$^{131}\text{I}$	$\beta$	0.6065	$234079 \pm 5$	96.64	3.22	0.14
$^{110\text{m}}\text{Ag}$	$\gamma$	0.6577	$48393 \pm 28$	88.07	4.36	7.57
$^{204}\text{Tl}$	$\beta$	0.76347	$84984 \pm 24$	96.60	2.96	0.44
$^{59}\text{Fe}$	$\gamma$	1.099	$39985 \pm 16$	95.98	1.52	2.50
$^{60}\text{Co}$	$\gamma$	1.332	$2207 \pm 3.4$	92.98	2.31	4.71
$^{86}\text{Rb}$	$\beta$	1.7792	$38677 \pm 23$	73.56	9.82	16.62
$^{90}\text{Y}$	$\beta$	2.288	$29563 \pm 19$	83.36	8.02	8.62
2. Metal Sources						
Cu XRF	Cu X-rays	0.008028	$22 \pm 0.8$			
Mo XRF	Mo X-rays	0.017374	$27 \pm 0.9$			
Ag XRF	Ag X-rays	0.021990	$30 \pm 1$			
$^{57}\text{Co}$	$\gamma$	0.1221	$6343 \pm 8.1$	88.18	5.71	6.11
$^{60}\text{Co}$	$\gamma$	1.332	$30123 \pm 34$			

Since both radioisotopes and XRF sources are involved in the study, energy of the most abundant radiation was taken as a common parameter to represent either one of the sources in Table I. It implies that 0.013336 MeV (of the abundant Rb  $\alpha_1\text{K L}_{II}$  X-ray) is mainly responsible for the 99.62% UV, 0.37% VIS, and 0.01% NIR radiation intensities of Rb XRF source. Similarly, the 0.514 MeV ( $E_{\text{max}}$  of abundant

$\beta$ ) is mainly responsible for the 96.81% UV, 0.85% VIS, and 2.34% NIR radiation intensities of  $^{137}\text{Cs}$ , though it also emits  $\gamma$ -rays and Ba X-rays. The UV, VIS, and NIR radiation intensity estimates of the sources provided complimentary information to what was obtained with optical filters on the nature of optical spectra. Dominant %UV intensity of the sources seen in Table I is due to presence of more number of peak intensity lines in spectral UV region (Fig.1). The data in Table I hinted the possibility of a linear relation between the UV, VIS, and NIR radiation intensities of the sources present as salts and the energy of their most abundant  $\gamma$ -, X-, or  $\beta$  radiation, when the sources are listed in increasing order of energy from 0.005 899 to 2.288 MeV. However, on plotting the data of Table 1 as shown in Fig.3, the linear relation between UV, VIS, and NIR radiation intensities and the energy of their most abundant  $\gamma$ -, X-, or  $\beta$  radiation became more evident. This key information helped ultimately in explaining the optical emission phenomenon. Low light yielding metal sources including Cu, Mo, and Ag XRF sources are shown separately as a group in Table I. Despite total opacity of metallic solids to light at room temperature, metal  $^{57}\text{Co}$  yielding 88.18% UV intensity close to 96.01% UV of the radiochemical  $^{57}\text{Co}$  exemplifies unusual optical properties of excited atoms situated on the metal surface.

### III. RESULTS AND DISCUSSION

#### A. Atomic spectra of solid metal sources

It was not clearly understood why (1) radiochemicals; (2) Rb, and Ba XRF sources; and (3) metal  $^{57}\text{Co}$  commonly caused high-energy spectra. However, optical spectra of metal sources (Fig.1, Table I) provided some vital clues on the nature of spectra of radioisotopes and XRF sources, in general. First of all, the observed optical spectra of metal sources unprecedented at room temperature hinted involvement of a previously unknown phenomenon. Furthermore, the observed optical spectra of metal sources opaque to light excluded from being the familiar luminescence. Therefore, optical emission from excited atoms situated on the metal surface was thought to be the most likely possibility. In clear words,  $\gamma$ -, X-, or  $\beta$  radiation energy at keV or MeV level generates a low energy at eV level that is optical emission from within the parent excited atom of a radioisotope or XRF source [3-6].

In general, atomic spectra of radioisotopes and XRF sources exhibited two spectral features (1) UV dominance, and (2) dependence upon ionizing radiation energy. UV dominance can be evident from the peak values: 99.62% UV at 0.013 336 MeV (Rb XRF), and 98.03% at 0.05954 MeV ( $\gamma$ ,  $^{241}\text{Am}$ ) given in Table I. Though UV is predominant in general from ionizing radiation sources, %UV falls from 99.62% to 83.36% when energy of maximum abundant ionizing radiation increases from 0.013 336 MeV (Rb XRF) to 2.288 MeV (of  $\beta$ ,  $^{90}\text{Y}$ ) as can be seen in Table 1 & Fig.3. a. When %UV attains maximum, %VIS, and NIR radiation intensities will be correspondingly low, as can be seen in the cases of Rb XRF source (0.37%, 0.01%), and  $^{241}\text{Am}$  (1.91%, 0.06%). However, on plotting the spectral data of Table I in Fig.3, the plots (a, b, and c) provided further clues on the nature of ob-

served spectra. Fig.3 (a) has disclosed a low energy source gives rise to high %UV, regardless of the fact whether it emits  $\gamma$ , X, or  $\beta$  radiation. Fig.3 (b, and c) shows such a source emits correspondingly low %VIS, and %NIR radiation intensities. In comparison, the %UV dips to a significant level, not below 83.36% in any case, from a relatively high energy source. The percent fall in UV is compensated by raise in %VIS, and NIR radiation intensities. Fig.3 provides a set of percent UV, VIS, and NIR radiation intensity estimates at any given ionizing radiation energy. In conclusion, the nature of spectrum of any source is predictable from its ionizing radiation energy.

The UV dominant high-energy atomic spectra were found to be independent of atomic number  $Z$  of the radioisotope or XRF source concerned, unlike the case of the basic atomic spectra [9, 10]. For example, 0.1221 MeV could cause 96.01% UV from within excited  $^{57}\text{Co}$  atom, whereas 1.332 MeV did 92.98% UV from within excited  $^{60}\text{Co}$  atom, despite both the sources are of cobalt element. Likewise, 0.013 336 MeV could cause 99.62% UV from within excited Rb atom in Rb XRF source, whereas 1.7 792 MeV did just 73.56% UV from within excited  $^{86}\text{Rb}$  atom in  $^{86}\text{Rb}$ , though both the sources are of rubidium element. Atomic number  $Z$  yet plays a pivotal role in causing gross light intensity somewhat comparable to the familiar strong lines of the element concerned in basic atomic spectra. Rb XRF source,  $^{131}\text{I}$ , and  $^{137}\text{Cs}$  proved to be exceptional among the sources tested in displaying gross light intensities far exceeding the number of ionizing radiation emissions, when tested with a bare PMT and then with a scintillation counter. It could be due to the reason that rubidium, cesium and iodine exceptionally show strongest air wavelengths at 424.440 nm (Rb II), 780.027 nm (Rb I), 460.379 nm (Cs II), 894.347 nm (Cs I), and 804.374 nm (I I), in Ref. [9]. Unlike these strong wavelengths in spectral VIS and NIR regions, the current high-energy spectra in general showed strong wavelengths in UV region. Use of relatively higher energies than the conventional thermal energies in valence excitation seemed to be responsible for shifting of strongest lines to spectral UV region in the case of radioisotopes and XRF sources. Futuristic studies of simultaneously detectable X-ray and optical spectra of XRF sources, and pair of nuclear and optical spectra of radioisotopes may enable better understanding of energy levels of excited atoms.

Table 1 suggests that 99.36% UV, 0.58% VIS, and 0.06% NIR radiation intensities in the gross light intensity are specific to 0.2245 MeV ( $E_{\beta_{max}}$  of  $^{147}\text{Pm}$ ). However, Fig.3 clarified further that 0.2245 MeV energy is responsible for causing the 99.36% UV, 0.58% VIS, and 0.06% NIR radiation intensities, regardless of the type of radiation whether  $\gamma$ , X-ray or  $\beta$ . Therefore,  $\beta$  may not exhibit its familiar particle nature to be distinctly different from  $\gamma$ -, or X-ray within an excited atom. The insight may prove a way to resolve the long-standing puzzle on dual nature of electron. In Fig.3, the %UV, VIS, and NIR radiation intensities of  $^{241}\text{Am}$  matched better with 0.05954 MeV of 35% abundant  $\gamma$ -ray than with the 5.486 MeV energy of 85.2% abundant  $\alpha$ -particle [12, 13], suggesting that  $\alpha$ -particle may not have participated in the current phenomenon of optical emission.

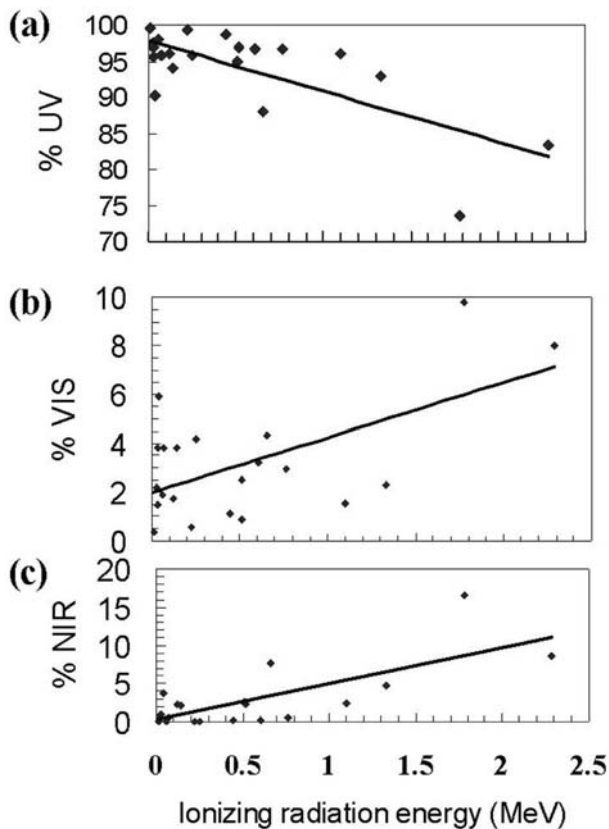


FIG. 3: The three plots (a, b, and c) made from spectral data of Table I disclose existence of a linear relation between ionizing radiation energy and the percent UV, VIS, and NIR radiation intensities in the gross light intensity. In other words, the nature of atomic spectrum of a radioisotope or XRF source is predictable as it depends upon energy of its abundant ionizing radiation. Fig. 3 (a) shows maximum UV radiation from both radioisotopes and XRF sources, and the %UV attains maximum at very low  $\gamma$ , X, or  $\beta$  radiation energy. Fig.3 (a, b, and c) shows as %UV decreases, the %VIS, and %NIR radiation intensities correspondingly raise. Extrapolation of the graphs shows  $\gamma$ , X, or  $\beta$  radiation sources with energy 14 MeV and above cause mostly visible (VIS), and NIR radiations. Some scattering of points seen in the graphs is due to ignoring the energies of less abundant emissions for sake of convenience.

### B. Atomic state of solid sources

Radioisotopes and XRF sources giving rise to high-energy atomic spectra of excited atoms has been confirmed by both the optical techniques (Figs.1 & 3). On the basis of atomic spectra of radioisotopes and XRF sources it is reasonable to believe the existence of free atoms in analogy to the thermally excited atoms in gaseous phase causing the basic atomic spectra [9, 10]. Mainly, during excitation to optical levels the excited atom may act as free atom without any bondage from surrounding unexcited atoms in a radioisotope or XRF source. Most importantly, formation of free atoms at room temperature owes to the generation of exciting energies within excited atoms, in wide contrast to the case of thermal energies from an external source in basic atomic spectra. For example, the 0.080 278 MeV (Cu  $K_{\alpha 1}$  X-ray) produced exciting energy is mainly responsible for formation of free Cu atoms

in Cu XRF source at room temperature. The excited free Cu atoms lying in between unexcited Cu atoms return to ground state not immediately following Cu X-ray emission but after the successive atomic emission of light. Similarly, in metal  $^{57}\text{Co}$  source, the 0.1221 MeV ( $\gamma$ ) produced exciting energy is mainly responsible for formation of free  $^{57}\text{Co}$  atoms, surrounded by unexcited Co atoms, as shown in Fig.4. In comparison, low abundant (33.4%) Fe  $K_{\alpha 1}$  X-ray energy fails to compete equally with 0.1221 MeV ( $\gamma$ ) in generating the free atoms in required number. Excited free  $^{57}\text{Co}$  atom returns to ground state as an unexcited Co atom not immediately after  $\gamma$ , and Fe X-ray emissions but after atomic emission of light (Fig.1, Table I). Formation of free atoms within solid radioisotopes and XRF sources implies existence of temporary atomic state of solids, regardless of temperature [3]. The duration of free atomic state is limited to valence excitation to optical levels resulting into fluorescence light emission. The free atoms behaving differently from thermally excited atoms in gaseous phase in basic spectroscopy are responsible for a new class of room temperature atomic emission spectra of solid radioisotopes and XRF sources.

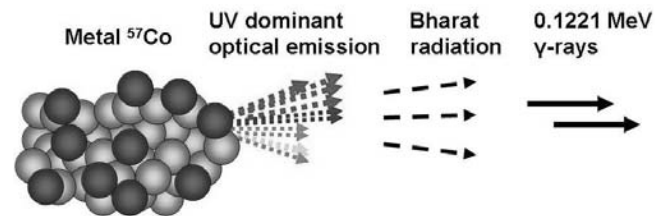


FIG. 4: Schematic of 0.1221 MeV  $\gamma$  rays followed by two successive generations: predicted exciting radiation (Bharat radiation) and the observed UV dominant optical emission at eV level from an excited  $^{57}\text{Co}$  atom in metal  $^{57}\text{Co}$  source. Valence excitation by  $\gamma$  produced Bharat energy enables the excited  $^{57}\text{Co}$  atoms to be free from surrounding unexcited Co atoms in ground state. The free excited atoms (shown in dark shade) that remain temporarily in atomic state of solids, regardless of temperature are responsible for the atomic spectrum of metal  $^{57}\text{Co}$  (Fig.1)

### IV. PREDICTED EXCITING ENERGY

Prior to the current study, as no previous literature is available either on ionizing radiation emissions causing fluorescent light emission from within an excited atom, or on theoretical prediction of the said emission, the author has attempted to provide the most plausible explanation [3-6]. In the first step towards this direction, a need arose to address the limitation that the ionizing radiations with keV or MeV energies known to knock out valence electron fail to do valence excitation to optical levels. The author has thus made a postulate that within an excited atom the ionizing radiations first

generate some exciting energy to be slightly higher than that of the observed UV at eV level, so that they do valence excitation resulting into UV emission. At the same time, it was verified whether the predicted energy really exists in electromagnetic spectrum. If  $\gamma$ -, X-, or  $\beta$  radiation truly generates the predicted exciting energy slightly higher than that of the observed UV, which in turn optical emission from within an excited atom, the exciting energy should occupy in between ionizing radiation and optical radiation in the electromagnetic spectrum. Since 0.010154 nm (0.1221 MeV) of the most abundant  $\gamma$ -emission is mainly responsible for the observed 330 nm peak wavelength of metal  $^{57}\text{Co}$  in Fig.1, the exciting wavelength should fall in between 0.010154 nm and 330 nm in the electromagnetic spectrum. However, since the basic cobalt spectrum [9] has minimum wavelengths 126.593 nm (Co II) in vacuum, it is very likely that exciting wavelengths from  $^{57}\text{Co}$  exist between 0.010154 to 126.593 nm. As no name exists for the range of wavelengths 0.010154 to 126.593 nm in between X-ray and optical spectral regions [9] of electromagnetic spectrum, the predicted radiation has been temporarily termed as Bharat radiation just for convenience [3, 6]. Citing the author's research work, Carlos Austerlitz et al described the role of Bharat energy and light produced following X-rays in exciting electron in their paper [11]. The wavelengths in the said range cannot be detected well by the currently available detector like photomultiplier tube. Figure 5 illustrates Rb X-ray spectrum followed by the experimentally observed UV dominant optical emission spectrum and the predicted wavelengths in between X-ray and optical spectra all from one and the same excited atom of Rb XRF source. Bharat wavelengths differ from one source to another. Most Bharat wavelengths exist between 0.010154 to 126.593 nm from  $^{57}\text{Co}$ , and between 12.87 nm and 47.488 nm from Rb XRF source (Fig. 5) in the electromagnetic spectrum.

## V. ATOMIC PHENOMENON

A brief phenomenological explanation comprising of two postulates is described in the following, so that a detailed mathematical explanation can follow later.

- (1) Ionizing radiation, particularly  $\gamma$ -, X-, or  $\beta$  radiation energy at keV or MeV level loses energy at eV level while passing through a core-Coulomb field. The loss of energy is reproduced as electromagnetic radiation with the same energy at eV level but higher than that of UV or EUV that the source emits.
- (2) The energy causes valence excitation resulting into UV dominant atomic spectrum.

The phenomenon is explained here in simple terms, keeping in mind that a detailed mathematical explanation can follow based on detailed spectral studies in future. Suppose gamma, X-ray or beta radiation with energy  $E$  is passing through M shell Coulomb field in an excited atom of a radioisotope or XRF source. According to the phenomenon described in Fig. 6, the radiation loses energy only by a few eV, so escapes from excited atom with the rest of the energy  $E_1$ . The loss of energy  $(E - E_1)$  reappears as exciting energy (Bharat energy),  $E_{BR}$ . The exciting energy  $E_{BR}$  depends upon

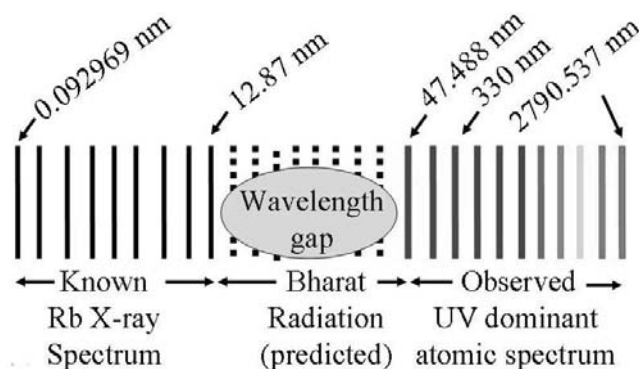


FIG. 5: Schematic of known Rb X-ray spectrum from Rb excited atom of Rb XRF source is shown on the left. The observed UV dominant optical emission spectrum generated by Rb X-rays from the same excited Rb atom is shown on the right. The 330 nm peak observed with narrow band optical filters in Fig.1 is expected to have caused by the highly abundant 0.092 969 nm ( $\alpha_1\text{K L}_{II}$ ) Rb X-ray. Therefore, the predicted wavelengths that do valence excitation and cause optical emission spectrum thus exist between the wavelengths 0.092 969 to 330 nm of the electromagnetic spectrum. However, since the basic rubidium X-ray spectrum ends at 12.87 nm, whereas optical spectrum begins at 47.488 nm (Rb II) in vacuum [9], Bharat wavelengths from Rb XRF source may exist between 12.87 and 47.488 nm in the electromagnetic spectrum. As these wavelengths cannot be called as X-rays or EUV, they were given the name Bharat radiation. Moreover, the wavelengths in this range cannot be detected well by the commercially available detector like photomultiplier tube

the initial ionizing radiation energy  $E$ , as explained already in the case of  $^{57}\text{Co}$ , and Rb XRF source.

$$E - E_1 = E_{BR}$$

The variation in %UV from one source to another can be explained by the phenomenon shown in Fig. 6. At low energy, the loss at eV level is relatively high while the  $\gamma$ -, X-, or  $\beta$  radiation passes through core- Coulomb field. For example, while 0.013 336 MeV ( $\alpha_1\text{K L}_{II}$  Rb X-ray) passes through a M shell Coulomb field in Rb XRF atom, probability exists to lose more energy, say, X eV, resulting in high energy Bharat photons at X eV. Moreover, as probability is high for such events to take place at low energies, the Bharat photons generated from Rb XRF source will be more in number. For these two reasons, the X eV Bharat photons from Rb XRF source have caused more peak intensity lines in spectral UV region, by valence excitation (Fig.1). In comparison, while 1.332 MeV energy passes through M shell Coulomb field in  $^{60}\text{Co}$  atom tend to lose relatively less energy, say, Y eV, resulting in low energy Bharat photons at Y eV. For this reason, the Y eV Bharat photons have caused more peak intensity lines in spectral VIS and NIR regions as compared to that of UV, by valence excitation (Fig.1). In clear words, X eV Bharat energy from Rb XRF source will be of higher energy than the Y eV Bharat energy from  $^{60}\text{Co}$ . The Bharat energies far exceeding thermal energies are responsible for the UV dominant optical emission observed, in general, from either a radioisotope or XRF source.

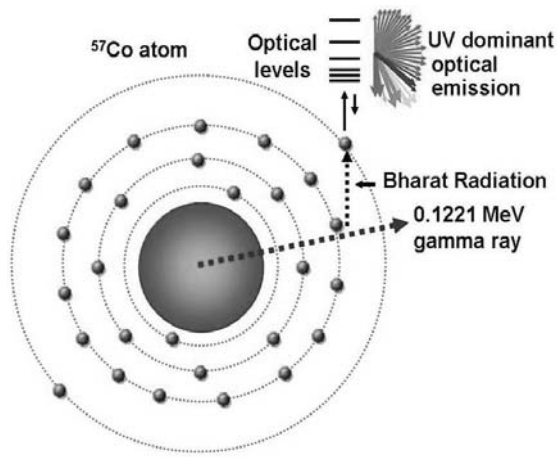


FIG. 6: Schematic diagram of a  $^{57}\text{Co}$  atom illustrating the phenomenon that generates some exciting energy higher than that of UV or EUV at eV level (termed temporarily as Bharat radiation). When the abundant 0.1221 MeV  $\gamma$ -ray passes through M shell Coulomb field loses energy at eV level only to reappear as Bharat energy with the same eV energy so as to be slightly higher than that of the observed UV or EUV. Typically Bharat energy internally produced within the  $^{57}\text{Co}$  excited atom excites the valence electron ( $4s^2$ ) and gives rise to room temperature UV dominant atomic spectrum shown in Fig.1.

#### A. Tritium: a source of Bharat radiation

The author was able to verify the validity of the phenomenon, when  $^3\text{H}$  did not show any optical emission on keeping a  $^3\text{H}$  ampoule directly on the quartz window of the bare PMT (9635QB Thorn EMI). The reason being  $^3\text{H}$  has only one electron, which is in K-shell. Passage of  $\beta$ -emission through K-shell Coulomb field generates a Bharat photon. However, in the absence of an electron in L-shell, the Bharat photon simply escapes from  $^3\text{H}$  atom without producing any light photon by valence excitation. Hopefully, this insight might prompt others to verify the author's experimental finding on  $^3\text{H}$ . Likewise, Bharat radiation emission alone takes place from highly ionized radionuclides left with a singly filled K shell that can happen in a situation like nuclear fission. Confirmation of this newly predicted Bharat energies higher than that of UV or EUV needs development of a PMT or some other detector sensitive enough in this energy region.

#### B. The phenomenon explains solar EUV

Findings of the current experimental study have a direct bearing on solar emissions. There is a similarity in the  $\gamma$ -, X-,  $\beta$ -, UV, VIS, and NIR radiation emissions from radioisotopes, XRF sources, and solar flares [14-19]. Therefore, the author has preliminarily reported [3] that solar  $\gamma$ -, X-, or  $\beta$  radiations cause EUV regardless of temperature by the atomic phenomenon described here. On the basis of the current study, it may be worthy of a review of interpretation of solar EUV lines to be of highly ionized atoms at high temperatures, and estimation of solar temperature from EUV line ratios [20-21].

An overall view of published reports suggesting presence of  $^{235}\text{U}$ ,  $^{238}\text{U}$ , and radioisotopes in solar flare indicate that the phenomenon described here could be the most likely cause for Solar EUV emission. For example, as detection of  $\gamma$ -, and neutron fission counts helps in finding the presence of uranium [22-23], simultaneous detection of X-rays,  $\gamma$ -rays, and neutrons reported in solar flares [24-27] suggests the presence of uranium in Sun. The hypothesis on likely presence of uranium in Sun derive further strength from the report on uranium content of solar salts [28] and traditional wisdom that  $^{235}\text{U}$  and  $^{238}\text{U}$  metals in the solar system are formed from previous supernovae. Moreover, presence of activation products such as  $^{56}\text{Co}$ , and  $^{24}\text{Na}$  in solar flare [29-32] and presence of  $^7\text{Be}$  in open air after a strong solar wind [33] need to be critically examined to see whether any possibility exists for Uranium fission in Sun. If fission truly happens, the fission fragments left over at the site of fission might constitute dark matter [3].

In the context of solar flare, the predicted Bharat radiation causing UV dominant optical radiation from radioisotopes and XRF sources by valence excitation seemed to be the familiar dark radiation from cosmic sources [3]. As Bharat energies produced internally within an excited atom cause non-thermal valence excitation resulting into UV emission from radioisotopes at room temperature, solar EUV may take place by valence excitation of dark energies from within excited atoms of radioisotopes present in solar flare regardless of temperature. As in the case of the current study, the  $\gamma$ -, X-, or  $\beta$  radiation emissions from radioisotopes formed by fission reaction in Sun cause two more generation of emissions: the predicted dark radiation, which is the same as Bharat radiation followed by EUV. Any how the current experimental study may prompt to examine all these possibilities.

#### C. UV in radiation dose data

Radiation dose data may need entry of UV as one more component, besides ionizing radiations in giving radiation dose to Nuclear Medicine patients administered with radio-pharmaceuticals such as  $^{99m}\text{Tc}$ ,  $^{131}\text{I}$ , and  $^{201}\text{Tl}$  for diagnostic and therapeutic purposes [6]. Since UV follows X-rays according to the current study, UV from diagnostic X-ray tubes may subject the patients to higher skin dose than previously thought. UV emission from metal  $^{60}\text{Co}$  may also contribute for the skin erythema noticed in cancer patients during  $^{60}\text{Co}$  Teletherapy treatment.

## VI. CONCLUSIONS

Hopefully, the current research may trigger new areas of research in the subjects of X-ray, nuclear, atomic, solar physics; and atomic spectroscopy. The UV dominant high-energy spectra of radioisotopes demonstrated with the commonly available laboratory sources meant for testing purposes may prompt detailed studies of atomic spectra of radioisotopes with higher strength to explain Solar EUV lines. It is worthy of examining whether  $^{235}\text{U}$  fission in Sun can be a viable alternative to the traditional fusion theory. Confirmation of the



predicted Bharat radiation or dark radiation requires improvement of PMT or some other detector to be sensitive enough to detect these energies between characteristic X-rays and EUV.

jasthan, India gratefully acknowledges his colleagues Dinesh Bohra, and Arvind Parihar for associating in initial experiments with black polyethylene sheet.

### ACKNOWLEDGEMENTS

The author, former Head of the Radiation Safety Group (Sc.E) at the Defence Laboratory (DRDO), Jodhpur, Ra-

- 
- [1] M. A. Padmanabha Rao, M. R. Patel, Beta excitation of a organic scintillator in powder form in *Luminescence: Phenomena Materials and Devices*, (Ed) R.P. Rao, Nova Science Publishers Inc., Commack, New York, 1992.
- [2] D. Bohra, A. Parihar, and M. A. Padmanabha Rao, *Nucl.Instrum.Methods.Phys.Res.* A320, 393 (1992).
- [3] M. A. Padmanabha Rao, in *Proc. 7th Int. Conf. on Human Ecology and Nature (HEN 2008)*, Moscow-Ples, Russia, 2008, edited by Vladimir V.Zaitsev (Moscow Scientific and industrial Association "Radon") p. 45.
- [4] M. A. Padmanabha Rao, Technical Report No: DLJ/IL/97/7\*, Defence Laboratory, Jodhpur- 342011, Rajasthan, India, 1997.
- [5] M. A. Padmanabha Rao, in *Proc. 12th National Symposium on Radiation Physics*, Defence Laboratory, Jodhpur, Rajasthan, India, 1998, edited by P. K. Bhatnagar and A .S. Pradhan (Hindusthan Enterprises: Jodhpur-342003, India, 1998) p. 273.
- [6] M. A. Padmanabha Rao. in *Proc. Symposium on Low Level Electromagnetic Phenomena in Biological Systems*, 1999, School of Environmental Sciences, Jawaharlal Nehru University, New Delhi, India, edited by Jitendra Behari, and Editors of *Indian Journal of Biochemistry and Biophysics* (Printed at National Institute of Science Communication, New Delhi- 110 012, 1999) p. 68.
- [7] H. Becquerel, *Comptes rendus de l' Academie des Sciences*, Paris,122, 501, (1890), translation in *Nuclear Chemistry, Benchmark papers in Physical Chemistry and Chemical Physics*, edited by G. T. Seaborg and W. Loveland (Hutchinson Ross Publishing Company, Pennsylvania, 1896) V.5, p. 23.
- [8] G. F. Knoll, *Radiation Detection and Measurement* (John Wiley & Sons, New York, 1979) p. 745.
- [9] David R. Lide and H. P. R Frederikse, *C.R.C. Handbook of Chemistry and Physics*, 74th Edition (CRC Press Inc, London, 1993-1994).
- [10] *Basic Atomic Spectroscopic data* (National Institute of Standards and Technology, Gaithersburg, U.S.A).
- [11] Carlos Austerlitz, Vivianne Lúcia Bormann de Souza, Diana Maria Tavares Campos, Cristina Kurachi, Vanderley Bagnato, and Cláudio Sibata, *Braz. arch. biol. technol.* 51, n.2, p. 271 (2008).
- [12] C. Michael Lederer and Virginia S. Shirley, *Table of Isotopes*, 7th Edition, (John Wiley & Sons, INC, New York, 1978).
- [13] *Radionuclide Transformations, Energy and Intensity of Emissions*, Report of a task Group of Committee 2, ICRP Publication 38 (Pergamon Press: Oxford, 1983).
- [14] S.R. Kane, in *Proc. the IAU Symposium No.68 on Solar Gamma, X-, and EUV radiation*, Buenos Aires, Argentina, 1974 (D. Reidel Publ. Co, Dordrecht, Holland, 1975) p. 446.
- [15] G. A. Doschek, in *Proc. IAU Symposium No.68 on Solar Gamma, X-, and EUV radiation*, Buenos Aires, Argentina, 1974 (D. Reidel Publ. Co, Dordrecht, Holland, 1975) p. 165.
- [16] Leon Golub, *Rev. Sci. Instrum*, 74, 4583 (2003)
- [17] Jeffrey W. Brosius and Kenneth J. H. Phillips, *Astrophys. J.*, 613, 580 (2004)
- [18] Alphonse C. Sterling and Ronald L. Moore, *Astrophys. J.*, 602, 1024 (2004).
- [19] Alphonse C. Sterling, in *Proc. Int. Astronomical Union 226 on Coronal and Stellar Mass Ejections*, Beijing, edited by K. Dere, J. Wang, and Y. Yan, 27, 2004 (Published Online by Cambridge University Press, 2005).
- [20] B. N. Dwivedi and Anita Mohan, *Solar Physics*, 156, no.1, 81 (1995).
- [21] E. E. Benevolenskaya, *Advances in Space Research*, 39, 1860 (2007).
- [22] Caldwell, Richard L, United States Patent 4568510, Dallas, TX, 1986.
- [23] E. E. Clark, Technical Report: K-2021-Suppl., Oak Ridge Gaseous Diffusion Plant, TN,USA,1981.
- [24] M. Yoshimori, K. Okudaira, Y. Hirasima, T. Igarashi, M. Akasaka, Y. Takai, K. Morimoto, T.Watanabe, K. Ohki, J. Nishimura, T. Yamagami, Y. Ogawara, and I.Kondo, *Solar Phys.*, 136, 69 (1991).
- [25] K. Watanabe, M. Gros, P. H. Stoker, K. Kudela, C. Lopate, J. F. Valdés Galicia, A. Hurtado, O. Musalem, R. Ogasawara, Y. Mizumoto, M. Nakagiri, A. Miyashita, Y. Matsubara, T. Sako, Y. Muraki, T. Sakai, and S. Shibata, *Astrophys. J.*, 636, 1135 (2006).
- [26] T. Sako et al., *ApJ*, 651, L69 (2006).
- [27] R. J. Murphy, Benzion Kozlovsky, G.H. Share, X-M Hua, and R.E. Lingenfelter, *ApJS*, 168, 167 (2007).
- [28] K. Ogiwara, T. Oi, T. Oosaka, M. Mukaida, and T. Honda, *J.Radioanal.Nucl.Chem*, 191, No.2, 273 (1995).
- [29] E. L. Chupp, D. J. Forrest, P. R. Higbie, A. N. Suri, C. Tsai, and P. P. Dumphy, *Nature*, 241, 333 (1973).
- [30] H. Nutley and M. D. Voth, *J.Geophys.Res.* 92:A10, 11179 (1987).
- [31] R.J. Murphy, X-M Hua, B Kozlovsky, and R. Ramaty, *Astrophys. J.*, 351, 299 (1990).
- [32] V. Tatischeff, B. Kozlovsky, J. Kiener, and R.J. Murphy, *astro-ph/0604325*, 2006.
- [33] C. Papastefanou and A. Ioannidou, *Applied Radiation and Isotopes*, 61, Issue 6, 1493 (2004).